Journal for ImmunoTherapy of Cancer

Vaccination generates functional progenitor tumor-specific CD8 T cells and long-term tumor control

Carlos R Detrés Román,[1] Megan M Erwin,[2] Michael W Rudloff,[2] Frank Revetta,[3] Kristen A Murray,[4] Natalie R Favret,[2] Jessica J Roetman,[1] Joseph T Roland,[5] Mary K Washington,[3] Mary Philip [6,7]

To cite: Detrés Román CR, Erwin MM, Rudloff MW, *et al*. Vaccination generates functional progenitor tumor-specific CD8 T cells and long-term tumor control. *Journal for ImmunoTherapy of Cancer* 2024;**12**:e009129. doi:10.1136/jitc-2024-009129

► Additional supplemental material is published online only. To view, please visit the journal online (https://doi.org/10.1136/jitc-2024-009129).

Accepted 30 August 2024

For numbered affiliations see end of article.

Correspondence to
Dr Mary Philip;
mary.philip@vumc.org

ABSTRACT

Background Immune checkpoint blockade (ICB) therapies are an important treatment for patients with advanced cancers; however, only a subset of patients with certain types of cancer achieve durable remission. Cancer vaccines are an attractive strategy to boost patient immune responses, but less is known about whether and how immunization can induce long-term tumor immune reprogramming and arrest cancer progression. We developed a clinically relevant genetic cancer mouse model in which hepatocytes sporadically undergo oncogenic transformation. We compared how tumor-specific CD8 T cells (TST) differentiated in mice with early sporadic lesions as compared with late lesions and tested how immunotherapeutic strategies, including vaccination and ICB, impact TST function and liver cancer progression.

Methods Mice with a germline floxed allele of the SV40 large T antigen (TAG) undergo spontaneous recombination and activation of the TAG oncogene, leading to rare early cancerous TAG-expressing lesions that inevitably progress to established liver cancer. We assessed the immunophenotype (CD44, PD1, TCF1, and TOX expression) and function (TNFα and IFNγ cytokine production) of tumor/TAG-specific CD8 T cells in mice with early and late liver lesions by flow cytometry. We vaccinated mice, either alone or in combination with ICB, to test whether these immunotherapeutic interventions could stop liver cancer progression and improve survival.

Results In mice with early lesions, a subset of TST were $PD1^+$ $TCF1^+$ TOX^- and could produce IFNγ while TST present in mice with late liver cancers were $PD1^+$ $TCF1^{lo/-}$ TOX^+ and unable to make effector cytokines. Strikingly, vaccination with attenuated TAG epitope-expressing *Listeria monocytogenes* (LM_{TAG}) blocked liver cancer development and led to a population of TST that were PD1-heterogeneous, $TCF1^+$ TOX^- and polyfunctional cytokine producers. Vaccine-elicited TCF1+TST could self-renew and differentiate, establishing them as progenitor TST. In contrast, ICB administration did not slow cancer progression or improve LM_{TAG} vaccine efficacy.

Conclusion Vaccination, but not ICB, generated a population of functional progenitor TST and halted cancer progression in a clinically relevant model of sporadic liver cancer. In patients with early cancers or at high risk of cancer recurrence, immunization may be the most effective strategy.

WHAT IS ALREADY KNOWN ON THIS TOPIC

⇒ Immunotherapy, including immune checkpoint blockade and cancer vaccines, fails to induce long-term remissions in most patients with cancer.

WHAT THIS STUDY ADDS

⇒ Hosts with early lesions but not hosts with advanced cancer retain a progenitor TCF1+tumor-specific CD8 T cell (TST) population. This population can be therapeutically exploited by vaccination, but not immune checkpoint blockade, to block tumor progression.

HOW THIS STUDY MIGHT AFFECT RESEARCH, PRACTICE OR POLICY

⇒ For people at high risk of cancer progression, vaccination administered when a responsive progenitor TST population is present may be the optimal immunotherapy to induce long-lasting progression-free survival.

INTRODUCTION

Immunotherapies such as immune checkpoint blockade (ICB) have reshaped the cancer treatment landscape, inducing long-term remissions in a subset of patients.[1] In contrast, while vaccines have been enormously successful in combating infectious disease, vaccines for non-viral cancers have had more limited success.[2] Most preclinical and clinical studies on tumor-specific CD8 T cell (TST) vaccine responses have been done in the context of established/late tumors.[3] Less is known about how TST respond and differentiate in response to immunotherapy during early stages of tumorigenesis when few cells harboring oncogenic mutations and potential neoantigens are present.[4]

We previously developed an autochthonous mouse model of liver cancer (AST;Cre-ER^{T2}) in which we could initiate liver carcinogenesis with tamoxifen (TAM)-induced Cre-mediated SV40 large T antigen (TAG) expression in hepatocytes.[5] TAG acts both as an oncogene, driving liver carcinogenesis,

and as a tumor-specific neoantigen recognized by CD8 T cells; this model allows precise temporal control of the duration of TST interactions with transformed hepatocytes and tumors. However, in contrast to human tumors, which arise sporadically and progress clonally,[4] TAM-induced oncogene induction is highly efficient, resulting in high antigen burden even in early-stage lesions. To better model sporadic cancer formation and subsequent progression, we allowed AST;Cre-ER^{T2} mice to undergo stochastic TAG oncogene activation through sporadic, TAM-independent Cre-mediated activity.

We found that TST in AST;Cre-ER^{T2} mice with early lesions upregulated PD1 and proliferated. Progenitor PD1+TST which express the transcription factor (TF) TCF1 and are localized in secondary lymphoid organs or tertiary lymphoid structures have been shown to maintain the TST population and mediate immunotherapy responses[6–9] and reviewed in Philip and Schietinger and Tooley *et al*.[10 11] In mice with early lesions, we found that a subset of PD1^{+} TST expressed the TF TCF1 and retained the ability to produce IFNγ. This subset was not sustained in mice with late lesions. Here, we tested whether immunization and/or ICB could improve TST function and found that immunization but not ICB generated a robust population of functional TST, which was able to halt and prevent long-term cancer progression in liver cancer-prone mice.

MATERIALS AND METHODS

Mice

All mice were bred and maintained in a specific pathogen-free barrier facility at Vanderbilt University Medical Center. TCR$_{TAG}$ transgenic mice (Strain 005236), Cre-ER^{T2} (Strain 008463), C57BL/6 (Strain 000664), and C57BL/6J Thy1.1 mice (Strain 000406) were purchased from The Jackson Laboratory. TCR$_{TAG}$ mice were crossed to Thy1.1 mice to generate TCR$_{TAG}$;Thy1.1 and TCR$_{TAG}$;Thy1.1/Thy1.2 (Thy1.12) mice. AST ((Albumin-floxStop-SV40 large T antigen) mice, obtained from Drs. Natalio Garbi and Günter Hämmerling, German Cancer Research Center and previously described,[12] were crossed to Cre-ER^{T2} mice to generate AST;Cre-ER^{T2}.

Tumor cohort setup

Age-matched and sex-matched AST;Cre-ER^{T2} were assigned to experimental tumor cohorts at 6 weeks of age. Both male and female mice were used for experimental cohorts. All tumor cohort mice were monitored twice weekly for body condition score (BCS) and abdominal distension (scored from 1 to 4: 1 no swelling, 2 mild abdominal enlargement, 3 moderate abdominal enlargement, 4 marked abdominal enlargement). Mice were analyzed at endpoint or specified time points as specified in figure legends and text. For survival studies, mice were euthanized at prespecified endpoints: (BCS 2), abdominal girth score 4, or difficulty with movement or eating/drinking. For intervention studies (*Listeria monocytogenes* (LM) vaccination and ICB), mice in AST;Cre-ER^{T2} tumor cohorts were randomly assigned to treatment arms. Sample size was determined to obtain 80% power to detect a 35% difference between groups, based on our previously observed/published differences and reproducibility. Potential confounders such as animal/cage location, treatment order, and measurement order were minimized by co-housing mice receiving different treatments. CRDR and MP were aware of the group allocation throughout experiments.

Liver tissue preparation, fixing and paraffin block

Liver tissue was removed from AST;Cre-ER^{T2} mice and immediately transferred into 10% buffered formalin for a minimum of 48 hours before transfer and storage in 70% ethanol. The Vanderbilt Translational Pathology Shared Resource performed paraffin embedding as follows: 70% ethanol for 30 min, 80% ethanol for 45 min, 95% ethanol for 45 min (twice), 100% ethanol for 45 min, 100% ethanol for 35 min (twice), xylene for 35 min (twice), wax (paraffin) for 60 min (three times).

Immunohistochemistry

SV40 TAG-specific mouse monoclonal antibody (BD Bioscience 554149) primary antibody was used. Antigen retrieval was performed with pH 6.0 citrate buffer at 105°C pressure cooker for 15 min and a 10 min bench cool down. Mouse on Mouse Ig Block was performed with Vector MKB-2213 and incubated for 60 min. Peroxidase block was performed at 0.03% H202 w/sodium azide and incubated for 5 min. Primary antibody was diluted at 1:800 and incubated for 60 min. Detection was performed with Dako EnVision+System HRP Labeled Polymer and incubated for 30 min. Chromogen was performed with DAB+ and incubated for 5 min.

Digital image analysis

Digital analysis of whole slide images was performed at the Digital Histology Shared Resources (VUMC). Whole slide images were captured on an Aperio AT2 slide scanner (Leica). Scripts were developed to quantify the number of TAG immunopositive (+) cells per tissue. The levels of DAB chromogen were extracted by color unmixing[13] from these whole slide images. Unmixed images were then processed with machine learning using the Ilastik software package[14] to produce probability maps of positive signal. Cells were identified and filtered by their size, location, and presence of a detectable nucleus. Positive cell counts were calculated per total number of cells and per tissue area.

Cell isolation

Spleens were mechanically disrupted to a single-cell suspension with the back of a 3 mL syringe plunger, passed through a 70 µm strainer and lysed with ammonium chloride potassium (ACK) buffer (150 mmol/L NH_4Cl, 10 mmol/L $KHCO_3$, 0.1 mmol/L Na_2EDTA). Cells were washed once and resuspended with RPMI-10: RPMI 1640 (Corning MT10040CV) supplemented with

10% FBS (Corning 35010CV). Livers were mechanically disrupted to a single-cell suspension using a glass pestle against a 150 µm metal mesh in cold PBS containing 2% FBS (2% FBS) and filtered through a 100 µm strainer. The liver homogenate was spun down at 400 g for 5 min at 4°C, and the pellet was resuspended in 15 mL 2% FBS, 500 U heparin (NDC 63323-540-05), and 10 mL PBS Buffered Percoll (Cytiva 17089102), mixed by inversion, and spun at 500 g for 10 min at 4°C. Pellets, enriched for liver-infiltrating lymphocytes, were lysed with ACK buffer, and cells were resuspended in RPMI-10 for downstream analysis. Periportal and celiac lymph nodes were collected and pooled for liver-draining lymph node (ldLN) analysis. Lymph nodes were mechanically dissociated into single-cell solutions using the textured surface of two frosted microscope slides into cold RPMI-10. Isolated leukocytes from spleen, lymph nodes, and liver were analyzed by flow cytometry as described below.

Adoptive T cell transfer

To transfer naive TCR_{TAG} T cells into AST;Cre-ER^{T2}mice, bulk splenocytes were sterilely isolated and processed from TCR_{TAG};Thy1.1 or TCR_{TAG};Thy1.12 transgenic mice as described above. To determine the number of CD8+Thy1.1+ or Thy1.12+TCR_{TAG}, an aliquot was taken from the single-cell splenocyte suspension after ACK lysis and counted via hemocytometer to obtain total splenocyte concentration and stained with antibodies for CD8, Thy1.1 and Thy1.12 Splenocytes were then resuspended in final volume of 200 uL of RPMI and injected intravenous into each recipient mouse. For experiments focused on early TST time points (60 hours to 21 days), 2.5×10^6 CD8+ TCR_{TAG};Thy1.1 and/or TCR_{TAG};Thy1.12 were injected per mouse in order to obtain sufficient numbers of cells across different cell divisions. For later immunization experiments where the goal was to reconstitute AST;Cre-ER^{T2} with a low number of naive TAG-specific T cell, we transferred 0.5×10^6 TCR_{TAG};Thy1.1/mouse.

Carboxy fluorescein succinimidyl ester labeling

Splenocytes were isolated and processed as described above and resuspended in 2.5 mL of RPMI. They were then rapidly mixed with equal volume of 2×carboxy fluorescein succinimidyl ester (CFSE) (10 µM) solution and incubated for 5 min at 37°C at a final CFSE concentration (5 µM). Stained cells were quenched by mixing with 5 mL pure FBS, washed twice with RPMI, and resuspended in 200 µL of RPMI for injection.

Listeria infection

LM ΔactA ΔinlB expressing Tag-I epitope (SAINNYAQKL, SV40 large T $antigen_{206–215}$) (LM_{TAG}),[5] or without exogenous antigens (LMΦ), were generated by Aduro Biotech and stored at −80°C. Mice were infected with 5×10^6 c.f.u. in 200 µL total volume of LM_{TAG} or LMΦ via intravenous injection.

Immune checkpoint blockade

Anti-PD1 (clone RMP1-14) and anti-PDL1 (clone 10.F.9G2) antibodies or isotype control (clone LTA-2) were purchased from BioXcell. Antibodies were diluted in 1X sterile PBS and injected in 200 µL total volume via i.p. injection every other day for five doses, at 200 µg per antibody per mouse.

Antibodies and reagents

Fluorochrome-conjugated antibodies and cell dyes were purchased from Miltenyi Biotech, Thermo, BioLegend, Tonbo/Cytek Biosciences, and Cell Signaling Technology. Specific antibodies are listed in table 1, and cell dyes are listed in table 2.

Splenocytes or liver-infiltrating lymphocytes from naive TCR_{TAG} mice or AST;Cre-ER^{T2} mice were stained with Ghost Dye Red 780 Viability Dye (1:2000 dilution) Tonbo/Cytek 13-0865 T500) and antibodies against surface molecules (CD8, Thy1.1, Thy1.12, CD44, PD1, LY108) in 2% FBS. Flow cytometry plots shown in figures are gated on

Table 1 Flow cytometry antibodies

Antibody	Fluorophore	Clone	Source	Identifier
Anti-CD8a	BV605	53–6.7	BioLegend	Cat# 100744
Anti-CD44	PcP-Cy5.5	IM7	Tonbo	Cat# 65-0441
Anti-CD44	FITC	IM7	BioLegend	Cat# 103006
Anti-Thy1.1	BV510	OX-7	BioLegend	Cat# 202535
Anti-Thy1.2	BV421	53–2.1	BioLegend	Cat# 140327
Anti-IFNγ	APC	XMG.12	BioLegend	Cat# 505810
Anti-PD1	APC	RMP1-30	BioLegend	Cat# 109112
Anti-TCF1	AF647	C63D9	Cell Signaling Technology	Cat# 6709S
Anti-TCF1	PE	C63D9	Cell Signaling Technology	Cat# 14456S
Anti-LY108	Pacific Blue	330-AJ	BioLegend	Cat# 134608
Anti-TNFα	PE	MP6-XT22	Life	Cat# 12-7321-82
Anti-TNFα	PE-Cy7	MP6-XT22	Biolegend	Cat# 506324
Anti-TOX	PE	REA473	Miltenyi Biotec	Cat# 130-120-716

Table 2 Flow cytometry cell dyes

Dye name	Source	Identifier
CFSE	Tonbo	Cat# 13-0850
Ghost Dye Red 780	Tonbo	Cat# 13-0865

Cell-surface and intracellular cytokine staining.
CFSE, carboxy fluorescein succinimidyl ester.

live CD8+Thy1.1+ or Thy1.12+transgenic TCR_{TAG}. The gating strategy is shown in online supplemental figure 1. For intracellular staining, splenocytes or liver-infiltrating lymphocytes were surface stained as above and then fixed and permeabilized using the FoxP3 TF Fix/Perm (Tonbo/Cytek TNB-0607) per the manufacturer's instructions before staining for intracellular molecules (TCF1, TOX, KI67). The samples were then analyzed by flow cytometry (see Flow cytometric analysis). For analysis of effector cytokine production (IFNγ, TNFα), ex vivo peptide stimulation was performed prior to staining. Bulk splenocytes or liver lymphocyte fractions were obtained as described above from naive or tumor-bearing AST;Cre-ER^{T2} mice and mixed with 2×10^6 C57BL/6 splenocytes and incubated in RPMI-10 for 4 hours at 37°C in the presence of brefeldin A (Biolegend 420601) and TAG peptide (SAINNYAQKL (0.5 µM); Genscript; custom-synthesized). The cells were then surface-stained (CD8, Thy1.1, Thy1.12), fixed and permeabilized as described above, stained with antibodies against IFNγ and TNFα and analyzed by flow cytometry.

Flow cytometric analysis

Flow cytometric analysis was performed using an Attune NxT four laser Acoustic Focusing Cytometer (ThermoFisher). Flow data were analyzed with FlowJo V.10 software (BD Biosciences).

Statistics

Survival curves were generated using the Kaplan-Meier method and compared using the log-rank (Mantel-Cox) test. For comparison of multiple survival curves, significance threshold was set using Bonferroni correction. For comparisons between two groups, Student's t-test was performed. For multiple comparisons, one-way or two-way analysis of variance (ANOVA) was performed, followed by either post hoc Tukey or Šidák test. The alpha level was set at 0.05. GraphPad Prism V.10 was used for all statistical analyses.

RESULTS

AST;Cre-ER^{T2} mice sporadically develop liver tumors which progress with age

We previously developed an autochthonous mouse model of liver cancer (AST;Cre-ER^{T2}) in which we can study TST interactions with cancer cells throughout carcinogenesis.[5] In AST;Cre-ER^{T2} mice, activation of Cre recombinase by a single dose of tamoxifen (TAM) induces expression of the SV40 large T antigen (TAG) under control of the albumin promoter/enhancer in hepatocytes. AST;Cre-ER^{T2} develop large liver tumors within 60–80 days post-TAM. To study tumor-specific CD8 T cell (TST) responses against TAG-driven tumors, we used congenic donor lymphocytes from transgenic mice in which CD8 T cells express a single T cell receptor (TCR) specific for TAG epitope-I (TCR_{TAG}).[15] We found that TST became dysfunctional in TAM-treated AST;Cre-ER^{T2} mice and were unable to halt tumor progression.[5] However, TAM-treated AST;Cre-ER^{T2} mice had a substantial tumor antigen burden, even at early stages of tumorigenesis, due to efficient TAM-induced Cre recombination. In most patients, oncogene activation occurs sporadically, thus we sought to determine how TST would differentiate and function in mice with rare sporadic transformed hepatocytes or early liver lesions.

In Cre-ER^{T2} mice, Cre recombinase can undergo stochastic tamoxifen-independent nuclear translocation,[16 17] putting hepatocytes in AST;Cre-ER^{T2} mice at risk of spontaneous TAG oncogene activation. Indeed, we found that as AST;Cre-ER^{T2} mice aged, they reproducibly developed liver tumors (figure 1A) and progressed to endpoint within ~225 days (figure 1B), much later than TAM-induced liver carcinogenesis. Liver tumors become grossly visible only after AST;Cre-ER^{T2} mice were >90 days, and mice >130 days had large tumors (figure 1A). For subsequent studies, we grouped 40–80 days aged mice without macroscopic liver lesions as "early", 90–120 days age mice with small visible tumors as "intermediate", and >130 days aged mice with large tumors as "late" liver lesion time points (figure 1A). We performed immunohistochemistry staining for TAG on livers from early, intermediate, and late AST;Cre-^{ERT2} mice. We used a machine learning algorithm (Ilastik)[14] to aid in identifying nuclei with positive signal, enabling us to quantify TAG nuclear expression in hepatocytes across scanned whole slide liver images. While early AST;Cre-ER^{T2} mice had rare small foci of TAG-positive hepatocytes, the percentage of TAG-positive hepatocytes progressively increased with time (figure 1A, right panel). The liver weight of AST;Cre-ER^{T2} mice increased due to tumor burden, with an initial slow growth phase followed by a more rapid growth phase (figure 1C).

TST are activated and proliferate in mice with early and late lesions

To compare initial TST differentiation in mice with early versus late liver lesions, we transferred CFSE-labeled naive TCR_{TAG} into early and late time point AST;Cre-ER^{T2} mice (figure 2A). TCR_{TAG} underwent extensive proliferation in mice with early or late liver lesions, upregulating PD1 as they divided (figure 2B, C). TCR_{TAG} in mice with early lesions divided more slowly, particularly in the spleen and ldLN (figure 2B, C), and there were fewer TCR_{TAG} in the spleens, ldLN, and livers of early mice as compared with late mice (figure 2D). The decreased TST proliferation in mice

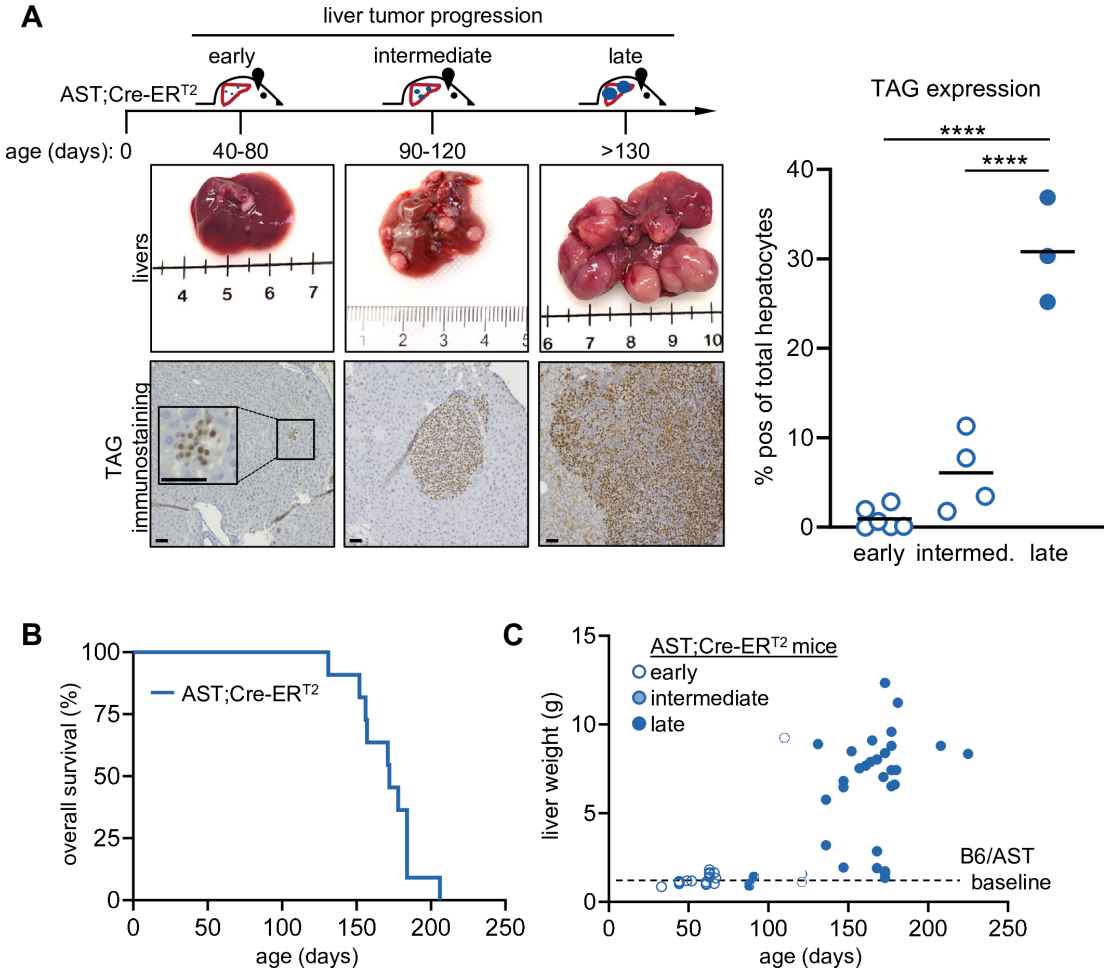

Figure 1 AST;Cre-ER^{T2} mice sporadically develop liver tumors with age. (A) Upper panel shows the timeline of tumor development in AST;Cre-ER^{T2} mice, with the middle panel showing corresponding gross liver images (measured in (cm)) and the lower panel showing TAG immunohistochemistry staining. Left, AST;Cre-ER^{T2} mice aged 40–80 days with grossly normal liver and few TAG+hepatocytes are classed as "early"; middle, aged 90–120 days mice with small macroscopic liver tumors and larger foci of TAG+hepatocytes are classed as 'intermediate'; right; >130 days mice with large tumors occupying most of the liver and large TAG+lesions are "late." Representative gross and TAG immunohistochemistry images of early, intermediate, and late AST;Cre-ER^{T2} mice are shown. Scale bar=50 µ. Right, percentage of total hepatocyte expressing TAG. Each symbol represents an individual mouse with n=3–6/group. ****p<0.0001 (one-way ANOVA with post hoc Tukey test). (B) Kaplan-Meier curve showing overall survival of AST;Cre-ER^{T2} mice across early, intermediate, and late time points, n=11. (C) Liver weights of AST;Cre-ER^{T2} male (n=59) mice plotted against age. Black dotted line shows baseline weights of tumor-free B6 and AST mice. ANOVA, analysis of variance.

with early lesions may be due to the lower TAG antigen burden (figure 1A); previous work has shown that TCR signal strength determines the speed and extent of T cell proliferation.[18] Within 60 hours of transfer, nearly all TCR_{TAG} in mice with late lesions and most TCR_{TAG} in mice with early lesions failed to produce effector cytokines TNFα and IFNγ (figure 2C). This is in line with our previous studies showing that transferred naive TCR_{TAG} fail to halt tumor progression.[5 19] Interestingly, in mice with early lesions, we identified a population of TCR_{TAG} in the spleen and liver that could produce effector cytokines TNFα and IFNγ (figure 2C). Thus, in hosts with sporadic early lesions, a subset of TST resisted rapid differentiation to the dysfunctional state, raising the possibility that this subset might be amenable to immunotherapeutic reprogramming/rescue.

A subset of TST remain functional in mice with early liver lesions

To determine whether this functional TST subset persisted, we examined TCR_{TAG} immunophenotype and function 5 days and 21 days post-transfer into early or late AST;Cre-ER^{T2} mice (figure 3A). As seen at the earlier 60 hours time point (figure 2D), fewer TCR_{TAG} were found in mice with early vs late lesions at 5 days post-transfer, however, the difference became less pronounced at 21 days (figure 3B). TCR_{TAG} in both early and late mice upregulated CD44, indicating antigen exposure and activation[20] (online supplemental figure 2). Notably, TCR_{TAG}

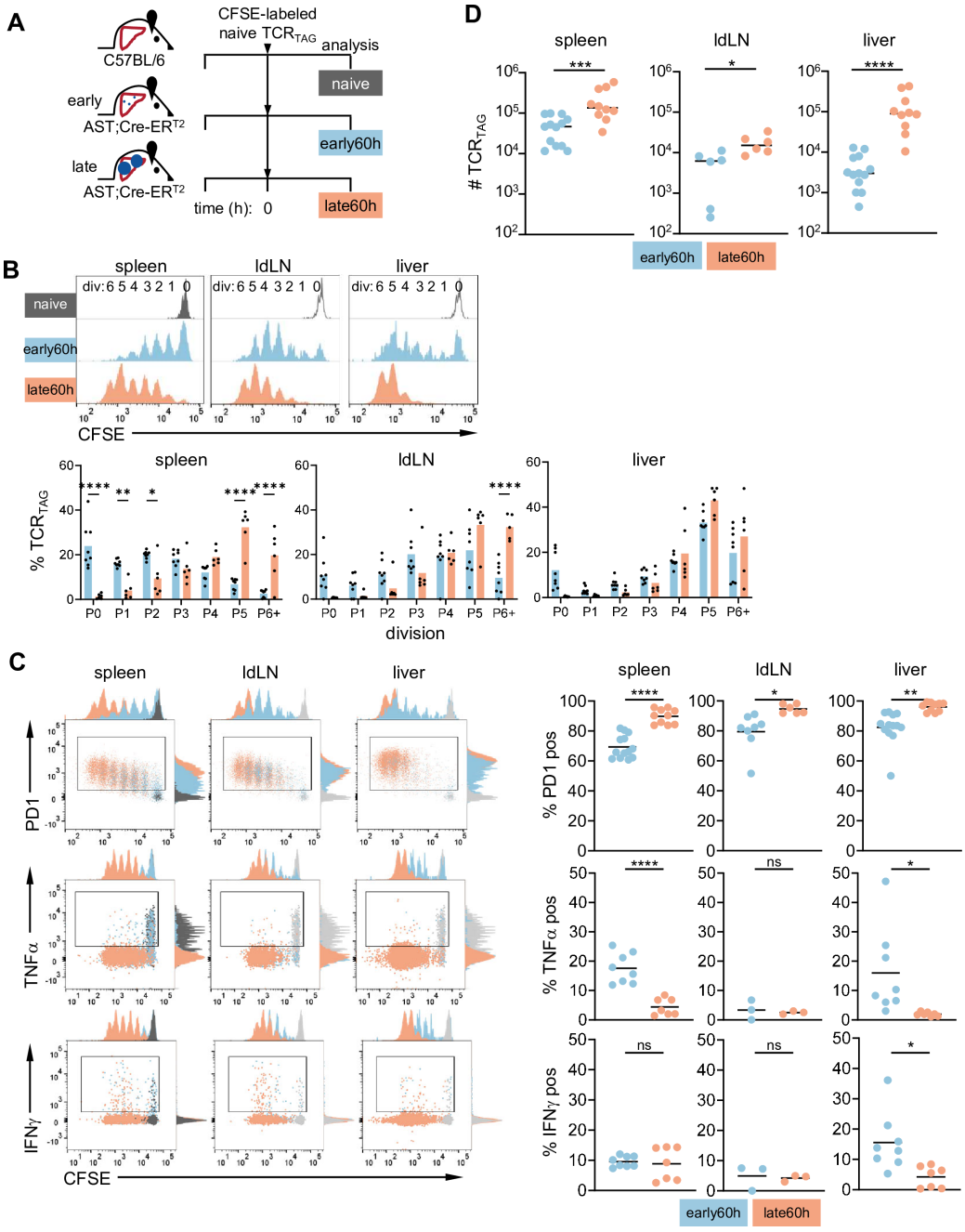

Figure 2 TST activate and proliferate in mice with early and late lesions. (A) Scheme: CFSE-labeled TCR_{TAG} were adoptively transferred into C57BL/6 (B6; naive, gray), early (blue) and late (orange) AST;Cre-ER^{T2} mice and analyzed 60 hours later. (B) Top, flow analysis of TCR_{TAG} CFSE dilution in the spleens, liver-draining lymph nodes (ldLN) and livers of early, late, and naive mice. This and all subsequent flow plots are gated on live CD8+Thy1.1+ cells (representative gating is shown in online supplemental figure 1A). Data are concatenated from three biological replicates and representative of three independent experiments. Bottom, percentage of TCR_{TAG} in each cell division for spleen, ldLN, and liver. Each symbol represents an individual mouse with n=6–8/group. *p<0.05, **p<0.01, ****p<0.0001 (two-way ANOVA followed by post hoc Šídák test). Biological replicates from two independent experiments were combined. (C) Left, PD1 expression directly ex vivo, and TNFα/IFNγ production after ex vivo TAG peptide stimulation, plotted against CFSE dilution. Naive T cells were assessed only from the spleen and shown as dark gray histograms or dots, naive T cells from the spleen are shown again in light gray in the ldLN and spleen plots for reference. Data are concatenated from three biological replicates and representative of two independent experiments for spleens and livers, and one experiment for ldLN. Right, percentage of TCR_{TAG} positive for PD1, TNFα and IFNγ. Gates for this and subsequent cytokine production figures were set based on no peptide stimulation controls. Each symbol represents an individual mouse with n=7–8/group for spleen and liver and n=3/group for ldLN. ns=not significant, *p<0.05, **p<0.01, ****p<0.0001 (unpaired Student's t-test). (D) Number of TCR_{TAG} in spleens, ldLN, and livers of early and late mice. Each symbol represents an individual mouse with n=10–13/group combined from three independent experiments for spleens and livers, and n=6 combined from two independent experiments for ldLN. *p<0.05, ***p<0.001, ****p<0.0001 (unpaired Student's t-test). ANOVA, analysis of variance; CFSE, carboxy fluorescein succinimidyl ester.

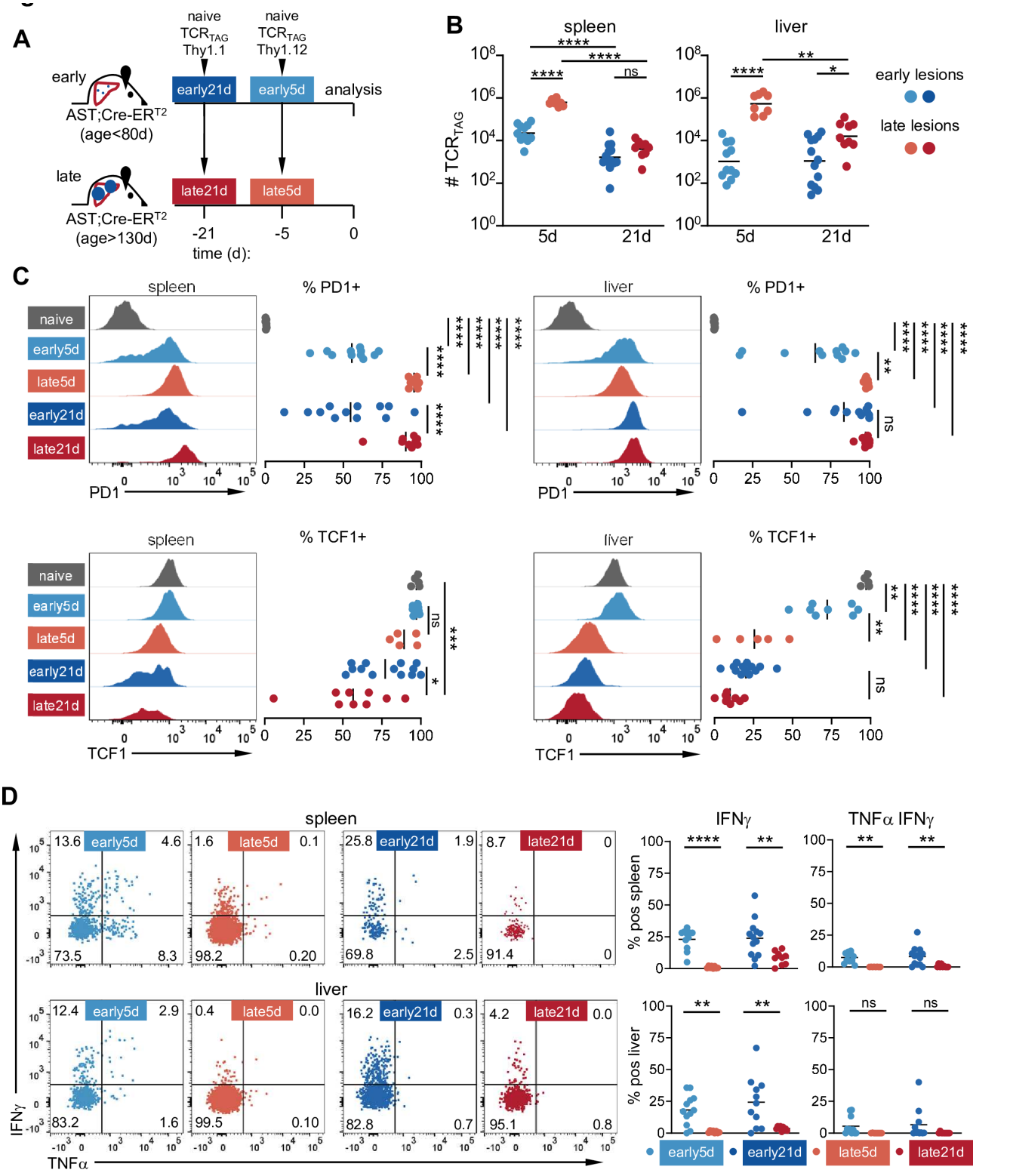

Figure 3 A subset of TST remain functional in mice with early liver lesions. (A) Scheme: TCR_{TAG} Thy1.1 were transferred into early (dark blue) and late (dark red) AST;Cre-ER^{T2} mice 21 days prior to analysis, followed by TCR_{TAG} Thy1.12 cells 5 days (light blue, light red) prior to analysis. (B) Number of TCR_{TAG} in spleens and livers of early and late mice. *p<0.05, **p<0.01, ****p<0.0001 (two-way ANOVA with post hoc Tukey test). (C) Left, histograms of TCR_{TAG} PD1 (upper panels) and TCF1 (lower panels) expression. Right, percentage of PD1+ (upper panels) and TCF1+ (lower panels) TCR_{TAG} with positive gate set to exclude (PD1) or include (TCF1) naive TCR_{TAG} (gray). Each symbol represents an individual mouse. *p<0.05, **p<0.01, ***p<0.001, ****p<0.0001 (one-way ANOVA followed by post hoc Tukey test). (D) Left, TCR_{TAG} TNFα and IFNγ production after 4 hours ex vivo TAG peptide stimulation. Right, percentage of TCR_{TAG} positive for IFNγ and TNFα/IFNγ. **p<0.01, ****p<0.0001 (two-way ANOVA, followed by post hoc Šídák test). For B–D, each symbol represents an individual mouse with n=11–13/early group and n=8–9/late group and combined from three independent experiments. ANOVA, analysis of variance.

in early mice continued to express higher levels of PD1 than naive TCR_{TAG}, suggesting that PD1 expression can identify tumor-reactive TST even in hosts with early lesions (figure 3C, upper panels). TST which express the TF TCF1 and localize to secondary lymphoid organs or tertiary lymphoid structures have been associated with improved responsiveness to immunotherapy[6–9] (reviewed in Philip and Schietinger and Tooley *et al*[10 11]). In contrast, TCF1- TST, predominantly found in the tumor, are resistant to therapeutic reprogramming.[19] At 21 days, TCR_{TAG} in early mice expressed higher levels of TCF1 in the spleen than late mice, while in the liver TCR_{TAG} in both early and late mice were TCF1-/low (figure 3C, lower panels) and TOX+ (online supplemental figure 2, lower panels); TOX is a TF associated with terminally differentiated TST.[21–25] While nearly all TCR_{TAG} in mice with late lesions were dysfunctional and failed to produce effector cytokines, mice with early lesions retained a subset of IFNγ-producing TCR_{TAG}, even at 21 days (figure 3D). Few TNFα+IFNγ+TCR_{TAG} were found in the livers of mice with early or late lesions, suggesting that TST dysfunction is more severe at the tumor site. These findings are in line with previous work in a mouse model of sporadic cancer arising in all organs which found that early immune tolerance was responsible for tumor progression.[26]

Vaccination early during tumorigenesis halts cancer progression

We next asked if the functional TST subset present in mice with early lesions could be harnessed to stop tumor progression. LM is a gram-positive intracellular bacterium which induces strong CD4 and CD8 T cell responses.[27] Using an *actA inlB* deficient attenuated LM vaccination strain,[28] which has been used in human clinical trials for advanced cancers[29–31] and engineered to express the TAG epitope I (LM_{TAG}),[5] we tested whether early vaccination of AST;Cre-ER^{T2} would protect mice from liver cancer progression. Young AST;Cre-ER^{T2} mice adoptively transferred with naive TCR_{TAG} and the following day were either left untreated (Φ), given a single dose of empty LM (LMΦ), or vaccinated with a single dose of LM_{TAG} and followed, with some cohorts analyzed prior to endpoint (figure 4A). LM_{TAG}-immunization conferred a major survival advantage, with all mice remaining tumor-free and one mouse euthanized for dermatitis without any evidence of liver tumors (figure 4B and online supplemental figure 3A). In contrast, mice in the Φ and LMΦ groups reached endpoint with multiple large liver tumors and increased liver weight (figure 4B, online supplemental figure 3B). At endpoint, most TCR_{TAG} in the LM_{TAG}-immunized mouse made effector cytokines, in contrast to the TCR_{TAG} in the tumor-bearing mice in the Φ and LMΦ groups which were largely unable to produce effector cytokines (online supplemental figure 3C), suggesting that functional TCR_{TAG} prevent liver tumor progression. For these studies, we adoptively transferred a lower number of naive TCR_{TAG} (5×10^5) for the purpose of reconstituting an endogenous population of TAG-specific CD8 T cells that could be followed longitudinally and targeted with interventions. Accordingly, early AST;Cre-ER^{T2} that received AT only or LM_{TAG} immunization only did not have improved survival as compared with untreated mice (online supplemental figure 3D), demonstrating that neither TCR_{TAG} nor LM_{TAG} alone were sufficient to halt tumor progression.

Progenitor TST are associated with vaccine efficacy

To determine whether the presence of functional TST correlated with later tumor-free survival, we analyzed TCR_{TAG} in Φ, LMΦ, or LM_{TAG}-vaccinated mice at age 100 days, before mice reached endpoint. Most TCR_{TAG} in the spleen and livers of Φ or LMΦ-treated mice failed to make effector cytokines (figure 4C), suggesting that without vaccination, the cytokine-producing TST observed at earlier time points (figure 3D) in mice with early lesions failed to persist long-term. In stark contrast, mice in the LM_{TAG} group had a large subset of double-producing $TNF\alpha^+IFN\gamma^+$ TCR_{TAG} in both the spleen and liver (figure 4C). LM_{TAG}-immunized mice had a larger population of TCR_{TAG} in the spleen (figure 4D), which were $PD1^-$ (figure 4E, left panel). Interestingly, there were two populations of TCR_{TAG} in the livers of LM_{TAG}-vaccinated mice, a $PD1^-$ and a $PD1^{int}$ population (figure 4E, right panel). LM_{TAG}-vaccinated mice had a higher number of TCF1+TOX- progenitor TST in the spleen and liver as compared with Φ and LMΦ-treated mice (figure 4F). While most TST in LM_{TAG}-vaccinated spleens were TCF1+TOX^-, in the liver there were two populations, a TCF1+TOX and a TCF1-TOX+ population (figure 4F, lower panel). Taken together, these data suggest that LM_{TAG} vaccination induces a robust population of functional TST, which sustains long-term antitumor responses, blocking cancer progression.

We next tested whether later vaccination could confer similar protection against liver tumor progression (figure 4G). Immunization at an intermediate time point (100 days), when few progenitor TST exist (Φ group, figure 4F), failed to slow liver tumor progression, and mice succumbed to tumors between 150 and 175 days, suggesting that progenitor TST are required for vaccine antitumor efficacy.

Vaccination is superior to ICB in blocking tumor progression

An important and open question in cancer immunotherapy is how ICB versus vaccination compares in boosting anticancer immune responses, and how best to combine and sequence these therapies.[2 32] Therefore, we compared the efficacy of ICB, LM_{TAG} vaccination, and combined ICB/ LM_{TAG} vaccination. Early AST;Cre-ER^{T2} mice adoptively transferred with TCR_{TAG} and then treated 30 days later with isotype control antibodies (iso), anti-PD1/anti-PD-L1 antibodies (ICB), LM_{TAG}, or combined LM_{TAG}/ICB (figure 5A). ICB conferred no benefit as compared with iso, with all mice developing large liver tumors (figure 5B, C). In contrast, LM_{TAG} and LM_{TAG}/

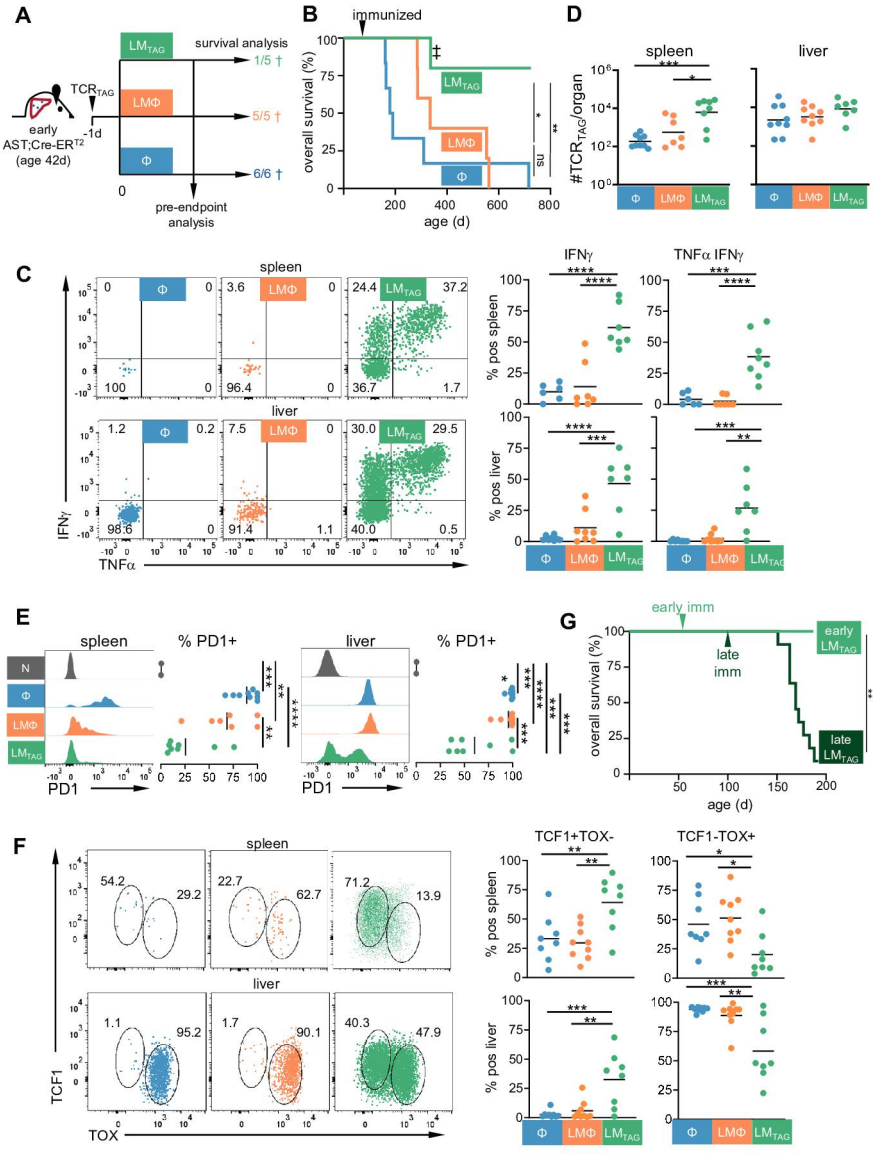

Figure 4 Early vaccination prevents liver tumor progression in AST;Cre-ER^{T2} mice. (A) Scheme: Early AST;Cre-ER^{T2} mice (42 days) were adoptively transferred with TCR_{TAG} and left untreated (Φ) or the following day, immunized with empty LM (LMΦ) or LM expressing the TAG antigen (LM_{TAG}). One cohort (survival analysis) was followed to humane endpoint and the second (pre-endpoint analysis) analyzed at age 100 days prior to tumor endpoint. The † and numbers indicate the number of mice in the long-term cohort who reached humane endpoint and were euthanized. (B) Kaplan-Meier curve showing survival of mice in each group with n=5–6/treatment group. *p<0.05, **p<0.01 (log rank (Mantel-Cox) test). The ‡ indicates a mouse euthanized for endpoint of severe dermatitis, whereas all other mice were euthanized due to advanced liver tumors. (C–F) Cohort as in A was euthanized and analyzed at age 100 days prior to tumor endpoint. (C) Left, TCR_{TAG} TNFα and IFNγ production after 4 hours ex vivo TAG peptide stimulation. Right, percentage of TCR_{TAG} positive for IFNγ and TNFα/IFNγ. Each symbol represents an individual mouse with n=6–7/group. **p<0.01, ***p<0.001, ****p<0.0001 (one-way ANOVA with post hoc Tukey test). (D) Number of TCR_{TAG} in spleen and livers. Each symbol represents an individual mouse with n=7–9/group. *p<0.05, ***p<0.001 (one-way ANOVA with post hoc Tukey test). (E) Left, histograms of TCR_{TAG} PD1 expression. Right, percentage of PD1+TCR_{TAG} with positive gate set to exclude naive TCR_{TAG} (gray). Each symbol represents an individual mouse with n=2 for naive and n=7–9 for other groups. **p<0.01, ***p<0.001, ****p<0.0001 (one-way ANOVA with post hoc Tukey test). (F) Left, TCF1 and TOX expression in TCR_{TAG}. Right, percentage of TCF1+TOX and TCF1-TOX+TCR_{TAG}. Each symbol represents an individual mouse with n=8–9/group. *p<0.05, **p<0.01, ***p<0.001 (one-way ANOVA with post hoc Tukey test). C–F shows samples pooled from two independent experiments. (G) Early AST;Cre-ERT2 mice (42 days) were adoptively transferred with TCR_{TAG} and immunized with LM_{TAG} 7 days later (early LM_{TAG}) or 60 days later (at age 110 days) (late LM_{TAG}). Kaplan-Meier curve showing survival of mice in each group with n=5–8/treatment group. **p<0.01 (log rank (Mantel-Cox) test). ANOVA, analysis of variance; LM, *Listeria* monocytogenes.

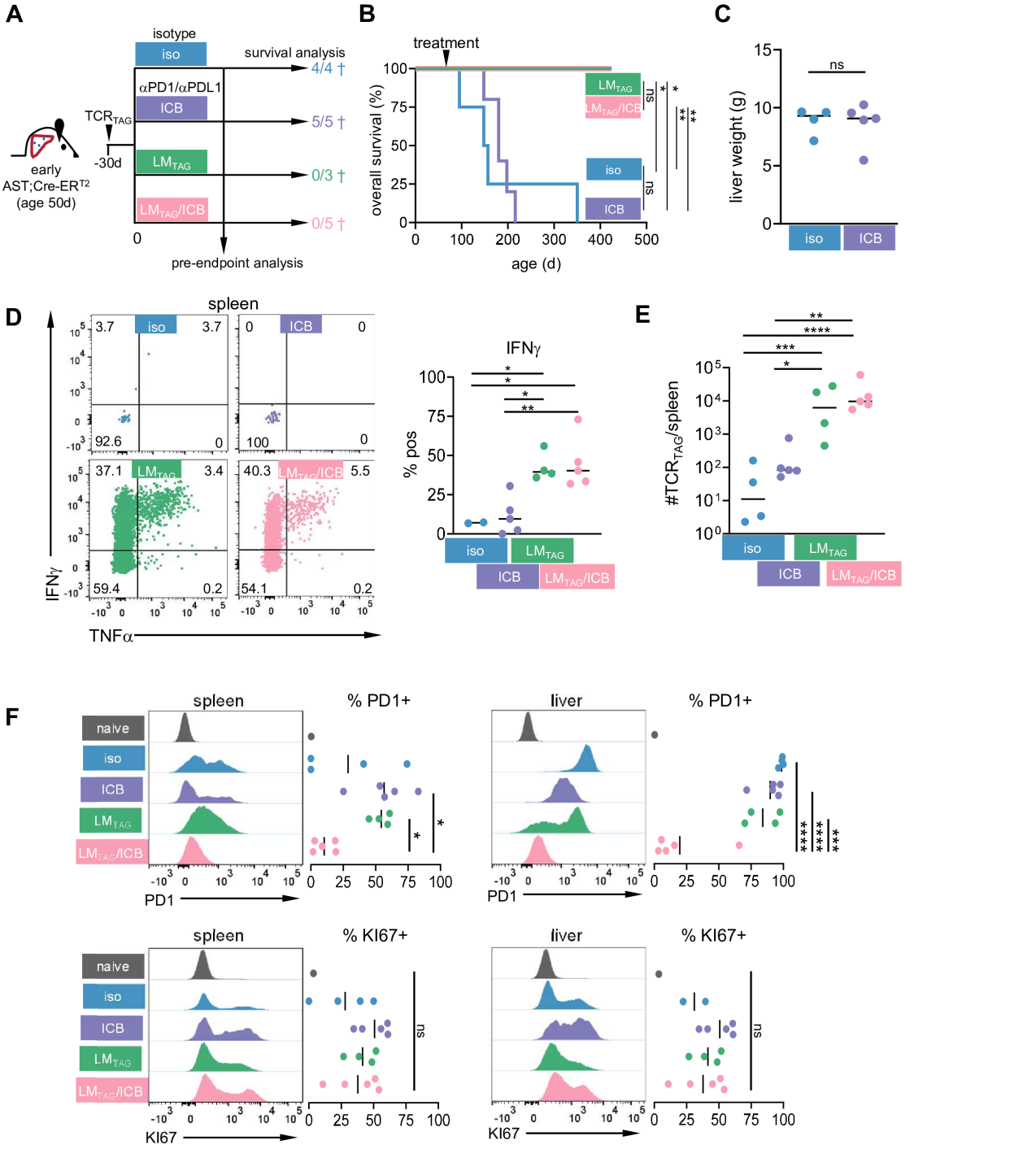

Figure 5 LM$_{TAG}$ vaccination is superior to immune checkpoint blockade (ICB) in preventing liver tumor progression. (A) Scheme: Early AST;Cre-ER^{T2} mice (50 days) were adoptively transferred with TCR$_{TAG}$ and treated 30 days later with isotype control antibody, anti-PD1/PDL1 antibodies (ICB), LM$_{TAG}$, or combination LM$_{TAG}$/ICB. One cohort (survival analysis) was followed to humane endpoint and the second (pre-endpoint analysis) was analyzed at age 90 days (on completion of ICB). The † and numbers indicate the number of mice in the long-term cohort who reached humane endpoint and were euthanized. (B) Kaplan-Meier curve showing survival of mice in each group with n=3–5/group. *p<0.05, **p<0.01 (log rank (Mantel-Cox) test). (C) Graph showing liver weights at humane end point. Each symbol represents an individual mouse, n=4–5/group. ns=not significant (unpaired Student's t-test). (D–F) Cohort as in A was analyzed at age 90 days prior to tumor endpoint. (D) Left, TCR$_{TAG}$ from spleen TNFα and IFNγ production after 4 hours ex vivo TAG peptide stimulation. Right, percentage of TCR$_{TAG}$ positive for IFNγ. Each symbol represents an individual mouse with n=2–5/group. *p<0.05, **p<0.01 (one-way ANOVA followed by post hoc Tukey test). (E) Number of TCR$_{TAG}$ in the spleen. *p<0.05, **p<0.01, ***p<0.001, ****p<0.0001 (one-way ANOVA followed by post hoc Tukey test). (F) Left, histograms of TCR$_{TAG}$ PD1 (upper panels) and KI67 (lower panels) expression. Right, percentage of PD1+ (upper panels) and KI67 + (lower panels) TCR$_{TAG}$ with positive gate set to exclude (PD1) or (KI67) naive TCR$_{TAG}$ (gray). Each symbol represents an individual mouse. *p<0.05, ***p<0.001, ****p<0.0001 (one-way ANOVA followed by post hoc Tukey test). ANOVA, analysis of variance; LM, *Listeria* monocytogenes.

ICB-treated mice had no evidence of tumor progression at 400+ days (figure 5B). We next analyzed TCR_{TAG} in iso, ICB, LM_{TAG}, or ICB/LM_{TAG}-treated mice at age 100 days. LM_{TAG} vaccination, either alone or in combination, led to a substantial increase in TST numbers and IFNγ production, while ICB alone had little impact (figure 5D, E and online supplemental figure 4A,B). Given the complete protection conferred by LM_{TAG} immunization alone, we could not evaluate the therapeutic contribution of ICB. However, the addition of ICB to LM_{TAG} did not improve TCR_{TAG} number or function (figure 5D, E and online supplemental figure 4A,B), even though ICB led to a decrease in PD1 surface staining (figure 5F), and there was a trend toward higher KI67, though not statistically significant (figure 5F). The disconnect between PD1 expression, proliferation, and effector function observed is in line with our previous observations on dysfunctional TST.[33] Interestingly, a study of combination therapy in a genetic mouse of pancreatic cancer found that in mice with detectable tumors, LM vaccination alone did not confer protection, while LM followed anti-PD1 ICB 21 days later did improve survival, though most mice eventually succumbed with tumors.[34]

LM_{TAG} immunization elicits a population of progenitor TST

Given that LM_{TAG} immunization and long-term tumor protection was associated with increased numbers of TCF1+TST in the spleen, we next explored the functional properties of these cells and their ability to self-renew and differentiate, the hallmarks of progenitor cells. We adoptively transferred early AST;Cre-ER^{T2} with TCR_{TAG} and immunized them 40 days later with LM_{TAG} (figure 6A). 60 days later, we sorted LY108+CD8+Thy1.1+TCR_{TAG} from the spleens, transferred them into secondary AST;Cre-ER^{T2} hosts and analyzed them 8 days later. LY108 is a widely used surrogate marker for TCF1 expression.[8] We first examined the correlation between TCF1 expression and functional capacity in the primary immunized hosts and found that cytokine-producing TCR_{TAG} were enriched for TCF1 expressors (figure 6B). Few TCF1-TCR_{TAG} produced cytokine, though not all TCF1+T-CR_{TAG} produced cytokine (figure 6B). Thus, TCF1 is not the sole determinant/predictor of function in this context. We next assessed LY108+TCR_{TAG} before and after sorting (figure 6C, D). The pre-sort TCR_{TAG} population in the spleen of LM_{TAG}-immunized mice was heterogeneous for TCF1 and TOX expression, though largely PD1-CD39-. LY108+TCR_{TAG} were uniformly TCF1+and heterogeneous for TOX expression. Eight days later, the progeny of transferred LY108+TCR_{TAG} were found in in higher numbers in the livers of 2° AST;Cre-ER^{T2} hosts (figure 6C, D). TCF1+TOX-TCR_{TAG} were present in the spleen, and a subset of TCR_{TAG} differentiated to a TCF1-TOX+terminally differentiated state, particularly in the liver. Moreover, TCR_{TAG} in the liver were largely PD1+CD39+, further evidence of tumor-driven terminal differentiation.[23] Thus, LY108+TCF1+ TCR_{TAG} elicited through LM_{TAG} immunization in tumor-prone mice behave as functional progenitor TST, capable of self-renewal and terminal differentiation in secondary hosts and protecting against tumor progression.

DISCUSSION

Here, we used an autochthonous liver cancer mouse model in which hepatocytes undergo spontaneous oncogene activation at a low frequency. With time, transformed hepatocytes progress from microscopic to small macroscopic to large late-stage liver tumors. Interestingly, while most TST activated in mice with early lesions upregulated PD1 and lost the ability to produce effector cytokines, a small subset of $TCF1^{+}$ TST persisted and retained the ability to produce IFNγ at early times post-transfer. Without intervention, this functional subset failed to persist, and the mice developed tumors. However, early vaccination in a genetic sporadic mouse model of liver cancer generated a large population of progenitor and polyfunctional TST, which blocked tumor progression and resulted in long-term survival. Given that the TAG oncogene is encoded in the germline, putting every hepatocyte at risk of transformation, this long-term protection is striking. In contrast, ICB treatment failed to confer protection from liver cancer progression or augment LM_{TAG} vaccination. Of note, later vaccination, at a time when the progenitor population was no longer present, failed to generate a polyfunctional population or block tumor progression.

The development and use of cancer vaccines is a key strategy to prevent or halt cancer progression and a main goal of the National Cancer Plan (https://nationalcancerplan.cancer.gov/about). LM-based vaccines have been tested in clinical trials with poor or mixed results.[27] These studies have mainly tested LM vaccines in patients with advanced or refractory cancers. Our studies could provide mechanistic insight as to why vaccine in patients with advanced cancers fail: for vaccines to be effective, a progenitor TST population must be present. We previously showed that over time and with continued tumor antigen exposure, the TCF1+TST population diminishes,[19] and there is increasing evidence that tumor burden negatively correlates with responses to ICB (reviewed in Dall'Olio *et al*[35]) and chimeric antigen receptor T cell therapy.[36] Hosts with early lesions and lower tumor antigen burden are more likely to harbor a population of progenitor TCF1+TST that respond to vaccination and protect against further tumor progression.

Our finding that vaccination blocked tumor progression while ICB did not may be surprising at first-glance, given that ICB is also known to act by recruiting progenitor TST to mediate antitumor responses.[37 38] An important point demonstrated by our results (figure 3 and figure 6) and previous studies is that not all TCF1+TST are functional, nor does ICB alone lead to functional TST.[19 39] TST activated in tumor-bearing hosts rapidly undergo widespread epigenetic remodeling, which is reinforced with continued tumor antigen exposure.[33] Removal from tumor[33] or PD-1

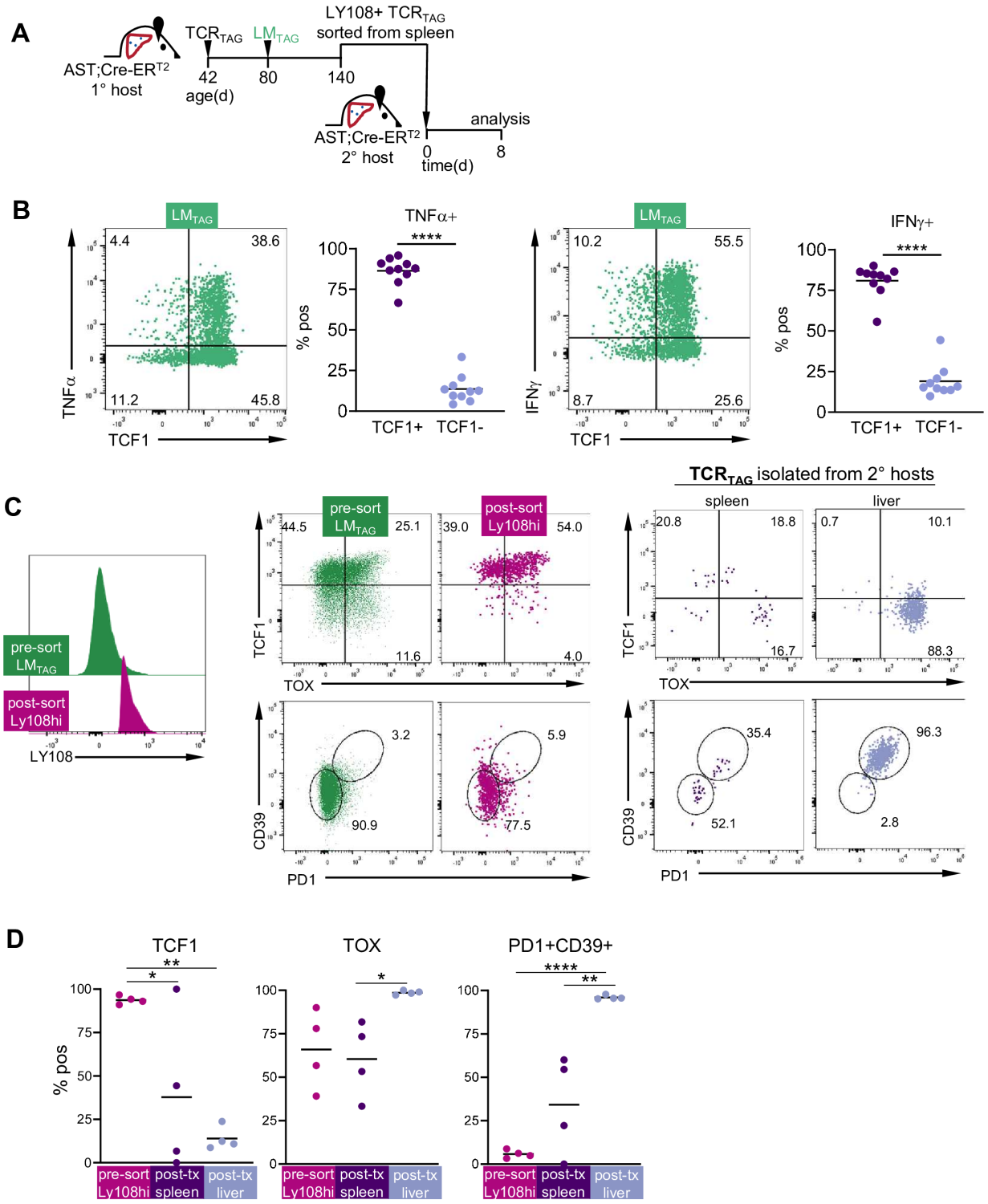

Figure 6 LM$_{TAG}$ immunization promotes the progenitor TST population. (A) Scheme Early AST;Cre-ER^{T2} were adoptively transferred with TCR$_{TAG}$ at age 42 days and immunized at age 80 days with LM$_{TAG}$. 60 days later, LY108+CD8+ Thy1.1+ TCRTAG were sorted from the spleen, transferred into secondary AST;Cre-ERT2 hosts and analyzed 8 days later. (B) Left, TNFα or IFNγ production after 4 hour ex vivo TAG peptide stimulation plotted against TCF1 in TCR$_{TAG}$ isolated from the spleens of LM$_{TAG}$-immunized 1° hosts. Right, percentage of TCF1 positive and negative cytokine-producing TCR$_{TAG}$. Each symbol represents an individual mouse with n=10/group. ****p<0.0001 (Student's t-test). (C) Left, LY108 expression of presort and postsort splenic TCR$_{TAG}$ from LM$_{TAG}$-immunized mice. Middle, TCF1 and TOX expression (top), and CD39 and PD1 expression (bottom) of presort and postsort LY108^{hi} TCR$_{TAG}$. Right, TCF1 and TOX expression (top), and CD39 and PD1 expression (bottom) from TCR$_{TAG}$ retrieved from spleen and liver of secondary hosts. (D) From left to right, percentage of TCF1+, TOX+, and PD1+CD39+ of presort LY108hi TCR$_{TAG}$ and post-transfer (tx) TCR$_{TAG}$ isolated from spleens or livers of secondary AST;Cre-ER^{T2}. For (C, D), n=4 primary and secondary hosts, representative of 2 independent experiments. *p<0.05, **p<0.01, ****p<0.0001 (one-way ANOVA followed by post hoc Tukey test). ANOVA, analysis of variance; LM, *Listeria* monocytogenes.

blockade[40] is not necessarily sufficient to reverse dysfunctional epigenetic reprogramming. Our findings suggest that LM_{TAG} vaccination, which provides antigenic stimulation in the context of an immunogenic pathogen, maintains/rescues functional progenitor $TCF1^+$ TST. Future studies will be needed to decipher mechanisms by which LM_{TAG} vaccination boost functional progenitor TST, why terminally differentiated TST fail to respond, and how different immunotherapies such as vaccines and ICB can be optimally combined. The sporadic liver cancer model we have developed and characterized provides an excellent platform for such future investigations, which could enable us to make long-term progression-free survival a reality for all patients with cancer.

Author affiliations
[1]Cancer Biology, Vanderbilt University School of Medicine, Nashville, Tennessee, USA
[2]Pathology, Microbiology, and Immunology, Vanderbilt University School of Medicine, Nashville, Tennessee, USA
[3]Pathology, Microbiology, and Immunology, Vanderbilt University Medical Center, Nashville, Tennessee, USA
[4]Medicine, Vanderbilt University School of Medicine, Nashville, Tennessee, USA
[5]Surgery, Vanderbilt University Medical Center, Nashville, Tennessee, USA
[6]Medicine, Vanderbilt University Medical Center, Nashville, Tennessee, USA
[7]Vanderbilt University Medical Center, Nashville, Tennessee, USA

X Mary Philip @philiplabvandy

Acknowledgements We thank the members of the Philip Lab and Dr. Andrea Schietinger for valuable feedback and discussion. We thank the Vanderbilt Division of Animal Care, the Vanderbilt Translational Pathology Core, the VUMC Tissue Morphology Core, and the Vanderbilt Digital Histology Shared Resource. We thank Dr Peter Lauer and Aduro Biotech (since acquired by Chinook Therapeutics) for providing attenuated Listeria strains.

Contributors Conception and design: CRDR, MME and MP. Experiments: CRDR, MME, MWR, KAM, FR, NRF and JJR. Analysis and interpretation of data: CRDR, JTR, MME, MKW, and MP. Writing of the manuscript: all authors. MP is the guarantor.

Funding This work was supported by the NIH through: R37CA263614 (MP), T32CA009592 (CRDR), T32GM008554 (NF), T32AR059039 (MME), T32GM007347 (MWR). Core services performed through Vanderbilt University Medical Center's Digestive Disease Research Center (DDRC) were supported by P30DK058404.

Competing interests None declared.

Patient consent for publication Not applicable.

Ethics approval All experiments were approved by the Vanderbilt University Medical Center (VUMC) Institutional Animal Care and Use Committee under protocol M1700166-02.

Provenance and peer review Not commissioned; externally peer reviewed.

Data availability statement Data are available on reasonable request. All data relevant to the study are included in the article or uploaded as online supplemental information. The data used and/or analyzed during the current study are available from the corresponding author on reasonable request.

ORCID iD
Mary Philip http://orcid.org/0000-0001-7496-2630

REFERENCES

1 Ribas A, Wolchok JD. Cancer immunotherapy using checkpoint blockade. *Science* 2018;359:1350–5.
2 Sellars MC, Wu CJ, Fritsch EF. Cancer vaccines: Building a bridge over troubled waters. *Cell* 2022;185:2770–88.
3 Philip M, Schietinger A. CD8+ T cell differentiation and dysfunction in cancer. *Nat Rev Immunol* 2022;22:209–23.
4 Willimsky G, Blankenstein T. The adaptive immune response to sporadic cancer. *Immunol Rev* 2007;220:102–12.
5 Schietinger A, Philip M, Krisnawan VE, *et al*. Tumor-Specific T Cell Dysfunction Is a Dynamic Antigen-Driven Differentiation Program Initiated Early during Tumorigenesis. *Immunity* 2016;45:389–401.
6 He R, Hou S, Liu C, *et al*. Follicular CXCR5- expressing CD8(+) T cells curtail chronic viral infection. *Nature New Biol* 2016;537:412–28.
7 Im SJ, Hashimoto M, Gerner MY, *et al*. Defining CD8+ T cells that provide the proliferative burst after PD-1 therapy. *Nature New Biol* 2016;537:417–21.
8 Utzschneider DT, Charmoy M, Chennupati V, *et al*. T Cell Factor 1-Expressing Memory-like CD8(+) T Cells Sustain the Immune Response to Chronic Viral Infections. *Immunity* 2016;45:415–27.
9 Wu T, Ji Y, Moseman EA, *et al*. The TCF1-Bcl6 axis counteracts type I interferon to repress exhaustion and maintain T cell stemness. *Sci Immunol* 2016;1:eaai8593.
10 Philip M, Schietinger A. Heterogeneity and fate choice: T cell exhaustion in cancer and chronic infections. *Curr Opin Immunol* 2019;58:98–103.
11 Tooley KA, Escobar G, Anderson AC. Spatial determinants of CD8+ T cell differentiation in cancer. *Trends Cancer* 2022;8:642–54.
12 Stahl S, Sacher T, Bechtold A, *et al*. Tumor agonist peptides break tolerance and elicit effective CTL responses in an inducible mouse model of hepatocellular carcinoma. *Immunol Lett* 2009;123:31–7.
13 Landini G, Martinelli G, Piccinini F. Colour deconvolution: stain unmixing in histological imaging. *Bioinformatics* 2021;37:1485–7.
14 Berg S, Kutra D, Kroeger T, *et al*. ilastik: interactive machine learning for (bio)image analysis. *Nat Methods* 2019;16:1226–32.
15 Staveley-O'Carroll K, Schell TD, Jimenez M, *et al*. In Vivo Ligation of CD40 Enhances Priming Against the Endogenous Tumor Antigen and Promotes CD8+ T Cell Effector Function in SV40 T Antigen Transgenic Mice. *J Immunol* 2003;171:697–707.
16 Heffner CS, Herbert Pratt C, Babiuk RP, *et al*. Supporting conditional mouse mutagenesis with a comprehensive cre characterization resource. *Nat Commun* 2012;3:1218.
17 Stifter SA, Greter M. STOP floxing around: Specificity and leakiness of inducible Cre/loxP systems. *Eur J Immunol* 2020;50:338–41.
18 Zehn D, Lee SY, Bevan MJ. Complete but curtailed T-cell response to very low-affinity antigen. *Nature New Biol* 2009;458:211–4.
19 Philip M, Fairchild L, Sun L, *et al*. Chromatin states define tumour-specific T cell dysfunction and reprogramming. *Nature New Biol* 2017;545:452–6.
20 DeGrendele HC, Kosfiszer M, Estess P, *et al*. CD44 activation and associated primary adhesion is inducible via T cell receptor stimulation. *J Immunol* 1997;159:2549–53.
21 Alfei F, Kanev K, Hofmann M, *et al*. TOX reinforces the phenotype and longevity of exhausted T cells in chronic viral infection. *Nature New Biol* 2019;571:265–9.
22 Khan O, Giles JR, McDonald S, *et al*. TOX transcriptionally and epigenetically programs CD8+ T cell exhaustion. *Nature New Biol* 2019;571:211–8.
23 Scott AC, Dündar F, Zumbo P, *et al*. TOX is a critical regulator of tumour-specific T cell differentiation. *Nature New Biol* 2019;571:270–4.
24 Seo H, Chen J, González-Avalos E, *et al*. TOX and TOX2 transcription factors cooperate with NR4A transcription factors to impose $CD8^+$ T cell exhaustion. *Proc Natl Acad Sci U S A* 2019;116:12410–5.
25 Yao C, Sun H-W, Lacey NE, *et al*. Single-cell RNA-seq reveals TOX as a key regulator of $CD8^+$ T cell persistence in chronic infection. *Nat Immunol* 2019;20:890–901.
26 Willimsky G, Blankenstein T. Sporadic immunogenic tumours avoid destruction by inducing T-cell tolerance. *Nature New Biol* 2005;437:141–6.

27 Oladejo M, Paterson Y, Wood LM. Clinical Experience and Recent Advances in the Development of *Listeria*-Based Tumor Immunotherapies. *Front Immunol* 2021;12:642316.
28 Sinnathamby G, Lauer P, Zerfass J, *et al*. Priming and activation of human ovarian and breast cancer-specific CD8+ T cells by polyvalent Listeria monocytogenes-based vaccines. *J Immunother* 2009;32:856–69.
29 Le DT, Brockstedt DG, Nir-Paz R, *et al*. A live-attenuated Listeria vaccine (ANZ-100) and a live-attenuated Listeria vaccine expressing mesothelin (CRS-207) for advanced cancers: phase I studies of safety and immune induction. *Clin Cancer Res* 2012;18:858–68.
30 Le DT, Wang-Gillam A, Picozzi V, *et al*. Safety and survival with GVAX pancreas prime and Listeria Monocytogenes-expressing mesothelin (CRS-207) boost vaccines for metastatic pancreatic cancer. *J Clin Oncol* 2015;33:1325–33.
31 Tsujikawa T, Crocenzi T, Durham JN, *et al*. Evaluation of Cyclophosphamide/GVAX Pancreas Followed by Listeria-Mesothelin (CRS-207) with or without Nivolumab in Patients with Pancreatic Cancer. *Clin Cancer Res* 2020;26:3578–88.
32 Enokida T, Moreira A, Bhardwaj N. Vaccines for immunoprevention of cancer. *J Clin Invest* 2021;131:e146956.
33 Rudloff MW, Zumbo P, Favret NR, *et al*. Hallmarks of CD8$^+$ T cell dysfunction are established within hours of tumor antigen encounter before cell division. *Nat Immunol* 2023;24:1527–39.
34 Kim VM, Blair AB, Lauer P, *et al*. Anti-pancreatic tumor efficacy of a Listeria-based, Annexin A2-targeting immunotherapy in combination with anti-PD-1 antibodies. *J Immunother Cancer* 2019;7:132.
35 Dall'Olio FG, Marabelle A, Caramella C, *et al*. Tumour burden and efficacy of immune-checkpoint inhibitors. *Nat Rev Clin Oncol* 2022;19:75–90.
36 Ventin M, Cattaneo G, Maggs L, *et al*. Implications of High Tumor Burden on Chimeric Antigen Receptor T-Cell Immunotherapy: A Review. *JAMA Oncol* 2024;10:115–21.
37 Miller BC, Sen DR, Al Abosy R, *et al*. Subsets of exhausted CD8$^+$ T cells differentially mediate tumor control and respond to checkpoint blockade. *Nat Immunol* 2019;20:326–36.
38 Siddiqui I, Schaeuble K, Chennupati V, *et al*. Intratumoral Tcf1+PD-1+CD8+ T Cells with Stem-like Properties Promote Tumor Control in Response to Vaccination and Checkpoint Blockade Immunotherapy. *Immunity* 2019;50:195–211.
39 Roetman JJ, Erwin MM, Rudloff MW, *et al*. Tumor-Reactive CD8+ T Cells Enter a TCF1+PD-1- Dysfunctional State. *Cancer Immunol Res* 2023;11:1630–41.
40 Pauken KE, Sammons MA, Odorizzi PM, *et al*. Epigenetic stability of exhausted T cells limits durability of reinvigoration by PD-1 blockade. *Science* 2016;354:1160–5.